

# Gain scheduled and robust $\mathcal{H}_\infty$ control above rated wind speed for wind turbines

Fredrik Sandquist<sup>a,\*</sup>, Michael Muskulus<sup>a</sup>, Olimpo Anaya-Lara<sup>b</sup>

<sup>a</sup>Department of Civil and Transport Engineering, Norwegian University of Science and Technology, Høgskoleringen 7a, 7491 Trondheim, Norway

<sup>b</sup>Institute for Energy and Environment, Department of Electronic & Electrical Engineering, University of Strathclyde, Royal College Building, 204 George Street, Glasgow, G1 1XW Scotland

---

## Abstract

This paper investigates two different approaches for individual pitch control for wind turbines. The first one is a gain scheduled decentralised control design and the second one is a robust  $\mathcal{H}_\infty$  loop shaping control design. Both controllers work well in the region above rated wind speed, exhibiting a response that is mostly independent of wind speed. The investigation is conducted based on the NREL 5MW benchmark wind turbine. Turbine modeling and control is conducted in FAST and Simulink.

© 2012 Published by Elsevier Ltd. Selection and/or peer-review under responsibility of SINTEF Energi AS.  
Open access under [CC BY-NC-ND license](https://creativecommons.org/licenses/by-nc-nd/4.0/).

*Keywords:* Wind Turbines, Individual Pitch Control, Load Mitigation

---

## 1. Introduction

With the increase in the size of wind turbines, as evident in the market penetration of multi-megawatt sized machines, there is increasing interest in exploiting the pitch control capabilities to alleviate fatigue loads. In addition to blade loads mitigation, the alleviation of tower fatigue loads has received special attention due to the fact that in offshore wind turbines the tower and foundations cost can account for roughly 40% of the total cost of the wind turbine.

For variable-speed wind turbines, the control regime is divided into an above-rated mode, where the task is to modify the blade pitch angle to regulate generator speed whilst maintaining rated power output, and a below-rated mode, where the task is to regulate generator speed between its minimum and maximum values to maximise power output (see figure 1).

Because of the increasing rotor size and the spatial load variations along the blade, it is necessary to react to turbulence in a more detailed way, with each blade separately controlled. Additional pitch control loops are sometimes included to damp the tower fore-aft motion or other structural vibrations in Region 3, [1–4]. The controllers designed in this paper are specifically designed to provide speed regulation in Region 3 in order to reduce the blade flap motions.

---

\*Corresponding author

Email addresses: [fredrik.sandquist@ntnu.no](mailto:fredrik.sandquist@ntnu.no) (Fredrik Sandquist), [michael.muskulus@ntnu.no](mailto:michael.muskulus@ntnu.no) (Michael Muskulus), [olimp.o.anaya-lara@eee.strath.ac.uk](mailto:olimp.o.anaya-lara@eee.strath.ac.uk) (Olimpo Anaya-Lara)

## 2. Wind turbine test model

The results presented in the paper correspond to the NREL 5 MW benchmark wind turbine [5]. The properties for the turbine are presented in table 1.

The dedicated software FAST [6], has been used for simulation and analysis of the wind turbine. The model in FAST is a structural dynamics model coupled with the aerodynamics simulation library Aerodyn [7]. The structural dynamics model is an assumed-modes model and the maximum degrees of freedom are 2 side-to-side tower modes, 2 fore-aft tower modes, 1 drive-train mode, 1 generator speed mode, 2 blade-flap modes for each blade, and 1 edgewise mode for each blade. The dynamic inflow model available in the Aerodyn user library has been used as opposed to the conventional blade element method. It was observed that both methods generate similar results provided the turbine works at typical tip-speed ratios. The dynamic inflow method gives incorrect results if the tip-speed ratio is small. A dynamic stall model has been used in the simulations.

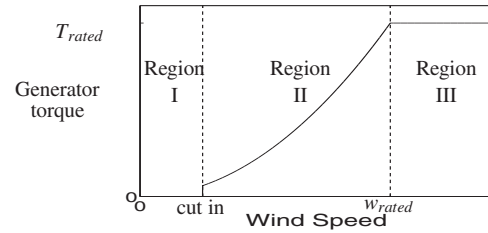


Fig. 1: Wind turbine operating regions

## 3. The wind turbine model

The wind turbine model has been Coleman transformed by the method explained in [4] and the Coleman system and Coleman coordinates, [8–10], are used in the rest of the paper. The subscripts  $c, h, v$  are used for the collective, horizontal and vertical Coleman coordinates respectively. A name convention used is that individual pitch/flap is used when talking about the horizontal and vertical Coleman coordinates for pitch/flap.

The model used in this paper has three inputs and three outputs.

$$\begin{bmatrix} \omega_g \\ f_h \\ f_v \end{bmatrix} = G \begin{bmatrix} \beta_c \\ \beta_h \\ \beta_v \end{bmatrix} \quad (1)$$

where  $G$  is the wind turbine model,  $\omega_g$  is the generator speed,  $f$  is the individual blade flap motions, i.e. collective blade flap is not used, [11], and  $\beta$  is the pitch input.

## 4. Linearization

The system has been linearized around different steady-state operating points in region 3. An operating point is given by a wind condition. A wind condition is parametrized by a uniform hub height wind speed, a linear or power law vertical wind shear and a linear horizontal wind shear. The linear wind turbine models depends quite a lot on the hub height wind speed but the difference between the linear models that corresponds to non zero wind shears compared to the linear model that corresponds to zero wind shears is small. Linear models with zero wind shears has been used in the rest of this article because of this. The wind speed range under study is between 12.1 m/s and 26 m/s. A singular value plot of two of the resulting linear systems can be found in figure 2a. Singular value plots for the same systems but only with the generator speed as output are shown in figure 2b, and only with flap motions as outputs are shown in figure 2c.

It is clear that the linear systems response depends on the mean wind speed, and the difference is large for the system with the generator speed as output, but not very large when the flap motions are the outputs. The difference in the gain to the generator speed can pose problems because the gain at low frequencies is much smaller at low wind speeds and the resonant peaks at higher frequencies are larger at low wind speeds.

Rating	5 MW
Rotor Configuration	Upwind, 3 blades
Control	Variable speed
Drive-train	High-speed gearbox
Rotor, Hub Diameter	126 m, 3 m
Hub height	90 m
Rated wind speed	11.4 m/s
Rated rotor speed	12.1 rpm
Rated Tip Speed ratio	7.55
Rated Tip Speed	80 m/s
Shaft Tilt, Precone	5, 2.5

Table 1: Properties for the NREL 5MW benchmark wind turbine

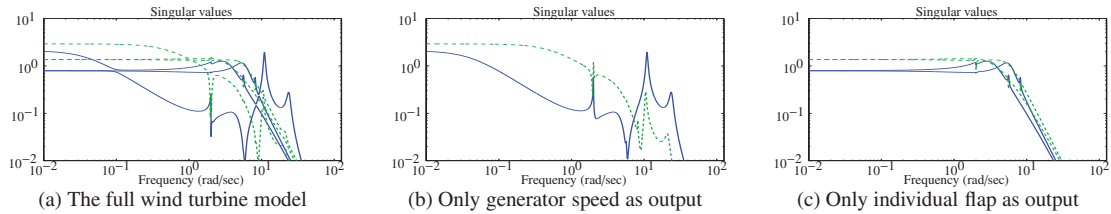


Fig. 2: Singular values plot for the wind turbine model at two different wind speeds. 12.1 m/s (solid) and 26 m/s (dashed)

### 5. Controller design

A controller designed with a wind turbine model linearized around a given wind speed, for example, 14 m/s, might work well at wind speeds close to 14 m/s but not in a wind speed of, for example, 20 m/s.

That problem can be approached by different methods. One common method is to design a gain scheduled controller, i.e., to design several different linear controllers for different operations points and change between them in a clever way. Another method is to design a robust linear controller, i.e., a controller that is designed to work in the whole operation region. Both these methods will be used in the remainder of the paper.

#### 5.1. Design of a base line controller

Previous work [11] suggests that it is possible to control the turbine with a simple decentralized controller, figure 3. The linear model at 14 m/s has been used when designing the baseline controller.

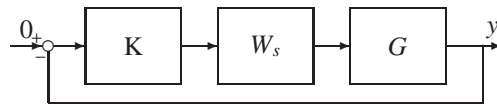


Fig. 3: The decentralized controller.  $K = \text{diag} \left( \begin{bmatrix} K_1 & K_2 & K_3 \end{bmatrix} \right)$  is a diagonal matrix of SISO controllers  $K_i$ .  $W_s$  is a static prefilter matrix.

#### 5.1.1. Diagonal controller

The Bode plot for the three control loops can be found in figures 4a and 4b (only one flap loop is shown but the other one is very similar).

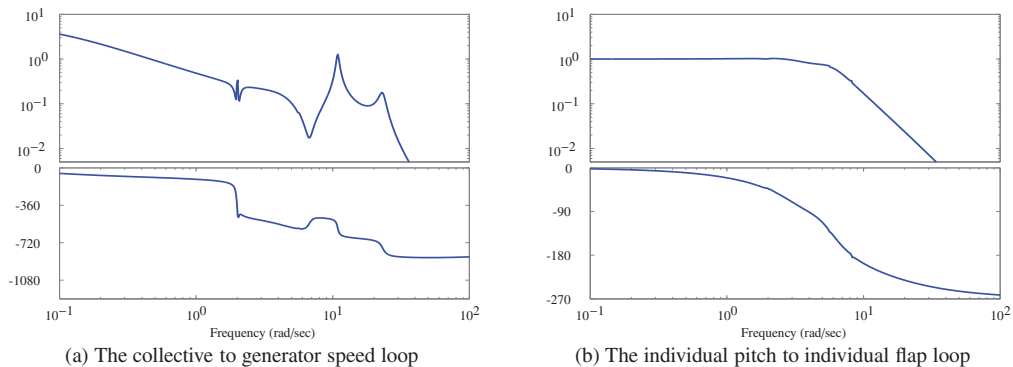


Fig. 4: Bode plots for the SISO loops at 14 m/s. The top row shows the amplitude of the transfer functions and the bottom row shows the phase of the transfer functions.

The individual pitch- individual flap loop is easy to control. The only problem is that the phase shift is relatively large, so it is necessary to advance the phase if fast control is desired. The collective pitch-speed loop response is harder to control because of low phase at low frequencies, a little bump in the magnitude at 2 rad/s, a very large phase shift at 2 rad/s and large resonances at 11 and 21 rad/s.

It is possible to use classical loop-shaping techniques on each loop. The controller design depends on how fast and robust the closed loop behavior must be. A PID controller for the individual pitch-individual flap loops has been used resulting in a bandwidth of 10 rad/s. The collective pitch-generator speed loop uses a PI regulator and two notch filters with zeros at the poles of the high-frequency resonances. The same PI controller without the notch filters results in more vibrations in the drive train. The bandwidth of this loop is about 1 rad/s. The diagonal controller performs satisfactorily and the individual flap motions is controlled very fast with a smooth response but the generator speed control is relatively slow.

### 5.1.2. The baseline controller at different wind speeds

The base line controller behaves well at wind speeds close to its design wind speed but behaves very badly at high wind speeds, see figure 9a. This can be fixed to some extent by using a slower controller but that would result in slow control at low wind speed which might not be satisfactory. A gain scheduled controller or more advanced robust controller might work better.

### 5.2. A Gain scheduled controller

The main control objective in region 3 is to control the generator speed to a constant reference value while the wind turbine is subject to changing wind conditions. The control is done by changing the pitch angles of the blades. A given wind condition defines an operation point  $OP_{w,p}$ , where  $w$  and  $p$  stands for the wind condition respectively the pitch input.

A simple gain scheduling approach to nonlinearities is to design a continuous set of linear controllers,  $K_{\alpha_j}(s)$ , that is parametrized by  $n$  scheduling variables  $\alpha_j$ ,  $j = 1, 2, \dots, n$ . A scheduling variable is a variable that can be measured or calculated from measured signals that determine what operation point the system works at or works close to. The controller output is then calculated by first calculating the scheduling variable,  $\alpha_j$ , and then using the controller  $K_{\alpha_j}(s)$  to calculate the output.

This control law is nonlinear and it is in general difficult to analyze the closed loop behavior. Simulations are often used to determine if the controller works well.

A gain scheduling controller can be designed by the following steps.

1. Determine continuous scheduling variables  $\alpha_j$ ,  $j = 1, 2, \dots, n$  that parametrize the continuous set of operation points.
2. Choose a discrete set of operating points  $OP^i$  and corresponding scheduling variables  $\alpha_j^i$ .
3. Choose a controller configuration that can be parametrized by the scheduling variables,  $K_{\alpha_j}(s)$ , for example a PID controller where the gain is a function of the scheduling variables.
4. Design controllers from the controller configuration chosen above,  $K_{\alpha_j}^i(s)$ , where  $i$  stands for the operation point, for each chosen operating point.
5. Define a continuous mapping from the scheduling variables to the set of controllers that give at least almost the designed controller for each chosen discrete operation point.

This method has been used for controlling the wind turbine by following the steps above.

1. An operating point  $OP_{w,p}$  was parametrized by the wind speed and pitch input. These are actually six parameters but the system is mostly nonlinear with regard to the mean wind speed so it is possible to only consider the operation points with zero wind shears and different mean wind speeds. Thus one wind parameter, the mean wind speed, is needed to determine the operating point. It can also be seen that the mean wind speed determine the collective pitch input because the generator speed is already given. So one mean wind speed  $w_u$  corresponds to one collective pitch input  $\beta_c$  (the vertical and horizontal pitch inputs are zero in a wind field with zero wind shear). It is thus possible to use either the mean wind speed or the collective pitch as a scheduling variable. The collective pitch is a very good measure of how much wind acts on the rotorplane. One drawback of using the collective

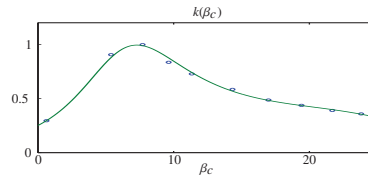


Fig. 5: The controller gain as a function of collective pitch. The circles show the gain for the operating points used in the calculation.

pitch is that it is one of the outputs from the controller and thus not independent of the controller. One drawback of using the mean wind speed is that (1) it needs to be measured and (2) that it might be difficult to measure it accurately and (3) a single measurement does not necessarily result in a good estimate of the total wind field that acts on the whole turbine. Thus the scheduling variable chosen is the collective pitch  $\beta_c$ .

- The operation points chosen and corresponding collective pitch inputs are

$$w^i = [12.1 \ 13 \ 14 \ 15 \ 16 \ 18 \ 20 \ 22 \ 24 \ 26] \text{ m/s} \quad (2)$$

$$\beta_c^i = [0.6 \ 5.4 \ 7.7 \ 9.6 \ 11.3 \ 14.3 \ 17.0 \ 19.4 \ 21.7 \ 23.8] \text{ degrees} \quad (3)$$

- Analysis of the transfer functions at the operation points shows that the base line controller designed in section 5.1 can be used by only changing the controller gain, i.e., the controllers is given by

$$K_{\beta_c}(s) = k(\beta_c)K_b(s) \quad (4)$$

where  $K_b(s)$  is the base line controller and  $k(\beta_c)$  is a scalar function of the collective pitch.

- The loop transfer function from collective pitch to generator speed for different operation points can be found in figure 6a.

It can be seen that the closed loop system is unstable or close to unstable for both low and high wind speeds. The problem at low wind speeds is that the phase is very low at low frequencies. The problem at high wind speed is that the system gain is higher than at the baseline wind speed and this result in a cross-over frequency that is too close to the natural frequency of the tower.

One possibly way to design the controllers for each operation point is to determine a new cross-over frequency for each operation point. Let us call the new cross-over frequencies  $\omega_c^i$ , where  $i$  stands for the operation point. A simple solution is to use the cross-over frequency for the baseline controller for wind speed above or equal to 14 m/s and a lower cross-over frequency for wind speeds below 14 m/s. It is also possible to determine the new cross over frequencies by determining a constant phase margin at all wind speeds.

The next step is to determine the controller gain,  $k(\beta_c^i)$ , to achieve these new cross-over frequencies. This can be achieved by calculating the gain of the loop transfer function at the new cross over frequency using the base line controller for all models,  $L(\omega_c^i)$ . The controller gain is now  $k(\beta_c^i) = 1/L(\omega_c^i)$ . The controllers for each discrete operation point have now been determined.

- Now we have a discrete function that determines the gain  $k(\beta_c^i)$  at each operation point, but it is necessary to have a continuous function  $k(\beta_c)$ . An easy way to achieve this is to assume that  $k(\beta_c)$  is a polynomial. It turns out that it is possible to achieve a good fit with a fourth order polynomial for the inverse relation  $k(\beta_c) = 1/k_p(\beta_c)$  where  $k_p(\beta_c) = c_0 + c_1(\beta_c) + c_2(\beta_c)^2 + c_3(\beta_c)^3 + c_4(\beta_c)^4$ . The parameters in the polynomial are determined by a least squares fit of the relation  $k_p(\beta_c^i) = 1/k(\beta_c^i) = L(\omega_c^i)$

Figure 5 shows the controller gain,  $k(\beta_c)$ .

Using the collective blade pitch as scheduling variable results in problems when determining the output from the controller. The control law is now

$$\beta_c = k(\beta_c)K(s)y \quad (5)$$

where  $K(s)$  is the baseline controller. This is an implicit equation in  $\beta_c$ . It is possible to solve this by at least two different methods. One method is to use a previous value of the collective pitch on the right hand side of the equation, i.e., to use the control law

$$\beta_c^t = k(\beta_c^{t-1})K(s)y \tag{6}$$

This can also be implemented by setting the  $k(\beta_c)$  before the controller  $K(s)$ , because the controller usually has a delay. Care needs to be taken for MIMO systems though. This results in slightly different results, because  $f(t)H(s)$  is not equal to  $H(s)f(t)$  when  $f(t)$  is a function of time.

Another method is to solve the equation for the collective pitch. This is easily done in our case by the use of a numerical solver. The two different methods gives almost equal results.

The loop transfer function with the use of gain scheduling can be found in figure 6b.

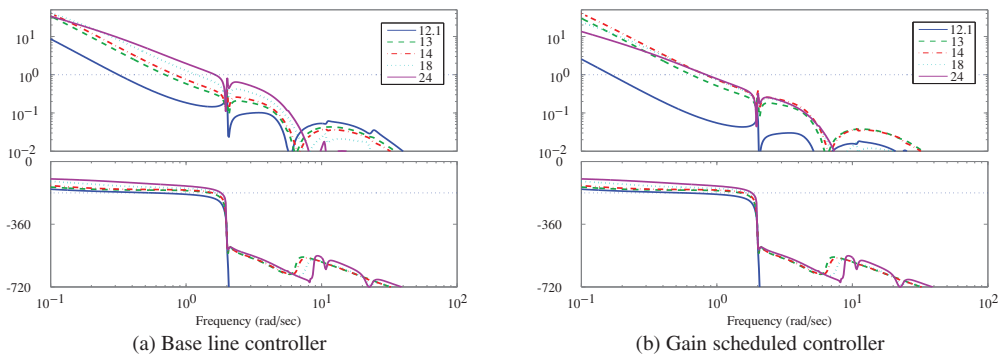


Fig. 6: The loop transfer function from collective speed to generator speed when the baseline controller respectively the gain scheduling controller is used for the models at 12.1, 13, 14, 18 and 24m/s

### 5.3. $\mathcal{H}_\infty$ loop shaping design

The gain scheduled diagonal controller designed in section 5.2 is simple to use but it might be difficult to achieve good closed-loop properties (such as high bandwidth and robustness). Another control method that has often resulted in good controllers is the  $\mathcal{H}_\infty$  loop-shaping procedure proposed in [12]. The method is also explained in detail in [13, 14]. The procedure is similar to a classic loop-shaping design, but it includes a second step after the loop-shaping is performed. The first step is to shape the singular values of the loop transfer function  $L_1 = W_2GW_1$ , with the use of a pre-filter  $W_1$  and a post-filter  $W_2$  (see figure 7).

The loop transfer function  $L_1$  is called the shaped plant. The goal of this step is to find filters  $W_1$  and  $W_2$  such that the shaped plant has a large magnitude where control is important, often at low frequencies, a crossover frequency that fits with the design, a roll-off-rate of about -1 around the crossover frequency to achieve stability, and enough roll-off at high frequencies to avoid problems with measurement noise and robustness. These requirements are similar to the requirements used in classical SISO loop-shaping design where the loop transfer function is shaped to achieve good control and good phase and amplitude margins. One important difference is that it is not necessary to consider closed-loop stability or stability margins in this step. This is especially good for MIMO systems because closed-loop stability might be difficult to achieve with loop-shaping for a MIMO system (and because the usual stability margins do not exist for MIMO systems).

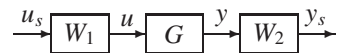


Fig. 7: The shaped plant

The second step is to robustly stabilize the loop transfer function  $L_1$  by a second controller  $K_r$  (see figure 8). This step is completely automatic and the complete controller  $K$  is then given by  $K = W_1K_rW_2$ . The controller  $K$  is going to have the same number of states as the shaped plant  $L_1$ .

The method is simple to use and often results in good controllers. A theoretical result is that the loop transfer function for the robustified shaped plant is relative close to the loop transfer function for the shaped plant, so the performance should be similar (similar crossover frequencies for example).

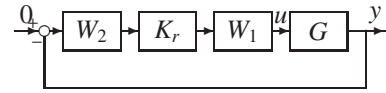


Fig. 8: Closed loop

One possible design procedure is to design the pre-filter as a decentralized PID controller with possibly some extra filters and then robustify that design. This procedure is used in this work and the controllers that have been robustified are the baseline controller and a faster version of the baseline controller. This method worked well on the wind turbine. These controllers also works in the whole region 3 as opposite to the base line controller that only works well close to its design wind speed. The design is also simpler to use as it is not necessary to take into account the closed-loop stability in the first design step. It is thus possible to get a good working design by the use of simpler loop-shaping filters. Note that the controller  $K$  depends on the scaling of the system, so proper scaling must be performed before the robustification step.

### 6. Simulations results

The different controllers have been tested in simulations. The simulation results presented in figure 9, are as follow: The first row shows the blade pitch angle in degrees, the blade flap at the tip in meters and the generator speed transformed via the gearbox to be similar in magnitude to the rotor speed in rpm. The second row shows the Coleman transformation of the pitch angle and blade flap, and the drive train angle in degrees. The third row shows the pitch rate in degrees per second, the tower back-and-forth and side-to-side displacements in meters, and the hub-height wind speed in m/s.

The simulation results for the baseline controller in a wind field with steps can be found in figure 9a. Figure 9b shows the simulation of the gain scheduled base line controller. Figure 9c show the robustified base line controller and Figure 9d shows a controller designed by the  $\mathcal{H}_\infty$  method based on a faster than the baseline diagonal controller.

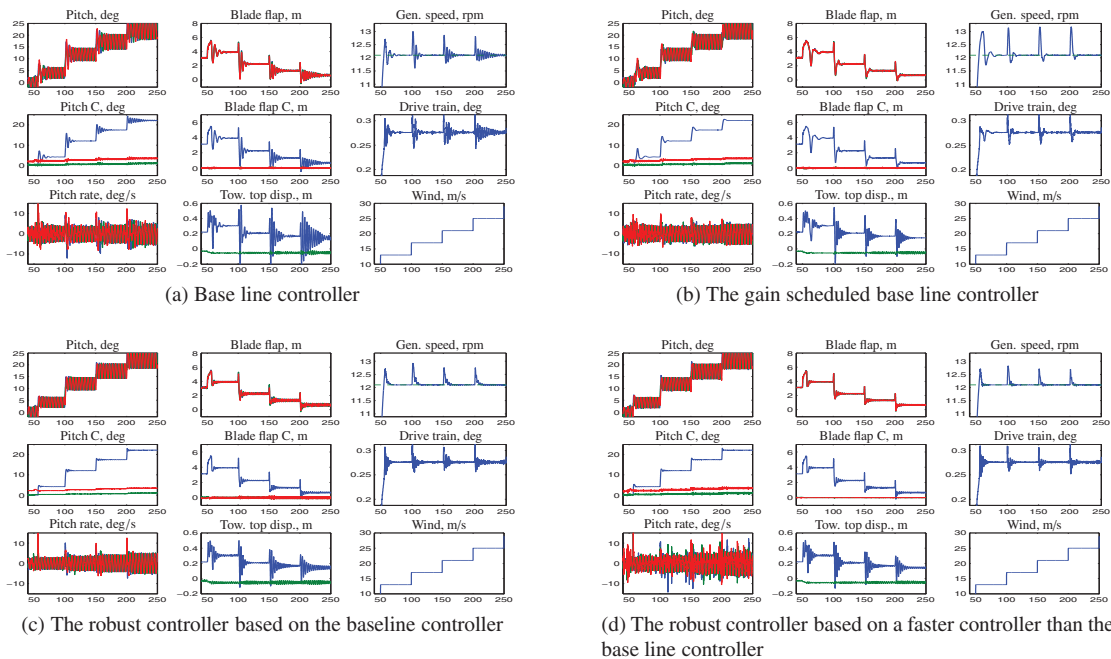


Fig. 9: Simulations with the controllers in a wind field with 4 m/s steps in the mean wind speed and a vertical power law wind shear of 0.3

The simulations show that the base line controller does not work well at high wind speeds because the responses in the blade flap, generator speed, drive train and tower motions have much larger oscillations at high winds speed compared to at lower wind speeds. The response of the gain scheduled base line controller seems to be mostly independent of the wind speed and the controller works well in the whole region 3. Both controllers based on the  $\mathcal{H}_\infty$  loop shaping design have a response that is mostly independent of the wind speed. The flap response of the  $\mathcal{H}_\infty$  loop shaping design based on the baseline controller is slightly worse compared to the response of the gain scheduled base line controller but the response for the generator speed is a little faster. The faster  $\mathcal{H}_\infty$  loop shaping design has a flap response that is faster compared to the other controllers but the generator speed response is similar to the response for the slower  $\mathcal{H}_\infty$  loop shaping design.

## 7. Conclusion

Two different individual pitch controllers that take into account the different behavior of a wind turbine at different wind speeds have been designed in this paper. The first one is a gain scheduled diagonal controller and the second one is a robust controller based on the  $\mathcal{H}_\infty$  loop shaping design method. Both controllers work well in the whole region 3. The gain scheduled controller is relatively easy to design, has a low order and the individual control loops are easy to understand. One possible drawback is that it is non linear. The  $\mathcal{H}_\infty$  loop shaping controller is easy to design but it gives a controller of a large order where the individual loops is difficult to understand.

## References

- [1] E. A. Bossanyi, Individual blade pitch control for load reduction, *Wind Energy* 6 (2003) 119–128.
- [2] P. Caselitz, W. Kleinhauf, T. Kruger, J. Petschenka, M. Reichardt, K. Storz, Reduction of fatigue loads on wind energy converters by advanced control methods, in: *Proceedings of the European Wind Energy Conference*, Dublin, 1997, pp. 555–558.
- [3] K. Selvam, Individual pitch control for large scale wind turbines, Tech. Rep. ECN-E-07-053, ECN (2007).
- [4] F. Sandquist, G. Moe, O. Anaya-Lara, Individual pitch control of horizontal axis wind turbines, *Offshore Mechanics and Arctic Engineering*, in press.
- [5] J. Jonkman, S. Butterfield, W. Musial, G. Scott, Definition of a 5-MW reference wind turbine for offshore system development, Tech. Rep. NREL/TP-500-38060, Golden, CO: National Renewable Energy (feb 2007 (to be published)).
- [6] J. Jonkman, NWTC Design Codes (FAST by Jason Jonkman), <http://wind.nrel.gov/designcodes/simulators/fast/> (Last modified 12-August-2005).
- [7] D. J. Laino, NWTC Design Codes (AeroDyn by Dr. David J. Laino), <http://wind.nrel.gov/designcodes/simulators/aerodyn/> (Last modified 05-July-2005).
- [8] M. Hansen, Aeroelastic stability analysis of wind turbines using eigenvalue approach, in: *Proceedings of the European Wind Energy Conference*, Madrid, 2007.
- [9] T. J. McCoy, Wind turbine ADAMS model linearization including rotational and aerodynamic effects, in: *Collection of the 2004 ASME Wind Energy Symposium Technical Papers at the 42nd AIAA Aerospace Sciences Meeting and Exhibit*, 2004, pp. 224–233.
- [10] D. J. Malcolm, Modal response of 3-bladed wind turbines, *Journal of Solar Energy Engineering* 124 (2002) 372–377.
- [11] F. Sandquist, G. Moe, O. Anaya-Lara, Decentralised control design for load mitigation in horizontal axis wind turbines (HAWTs), in: *OMAE 2011, 30th International Conference on Ocean, Offshore and Arctic Engineering*, 2011, p. 50147.
- [12] K. Glover, D. McFarlane, Robust stabilization of normalized coprime factor plant descriptions with  $\mathcal{H}_\infty$ -bounded uncertainty, *IEEE Transaction of Automatic Control* 34 (1992) 821–830.
- [13] S. Skogestad, I. Postlethwaite, *Multivariable feedback control, analysis and design*, John Wiley and Sons, LTD, 1996.
- [14] K. Zhou, J. C. Doyle, K. Glover, *Robust and optimal control*, Prentice Hall, 1996.